Numerical Study on the behavior of a biphasic temperature-sensitive hydrogel twisting actuator

Amir Ghasemkhani[1], Hashem Mazaheri [1]*,Pouya Beigzadeh Arough[1]
[1] Department of Mechanical Engineering, Bu-Ali Sina University, Hamedan, Iran.

Abstract
In this research, twisting behavior of a multi-layered hydrogel-based actuator which is comprised of two temperature-sensitive hydrogel layers and one elastomeric layer as the main core, is studied in different aspects due to the temperature changes. For this purpose, firstly, a suitable model for temperature-sensitive hydrogel is implemented in ABAQUS software by using UHYPER subroutine. Then, twisting behavior of the actuator is simulated due to temperature changes and both twisting angle and reaction torque are obtained for the actuators with different boundary conditions. To study the effect of different material and geometric parameters on the performance of under-study actuator, a comprehensive parameter study is conducted. These parameters include cross-linking density of the hydrogel, volumetric percentage of the hydrogel, geometry of interface line of the layers, and aspect ratio (cross-section dimensions) of the actuator. Considering the obtained results, the actuators with the maximum twisting angle and maximum reaction torque are recognized. Briefly, the reaction torque generated at the ends of the twisting actuator is maximum for the case where the interface line passes through the corners of the actuator cross-section. But the results show that for the maximum twisting angle of the under-study actuator, the so-called interface line should not pass through the actuator corners.
Keywords: Temperature-sensitive hydrogel, Hydrogel twisting actuator, Numerical simulation.

1) Introduction
Hydrogels are 3D polymer networks with covalent cross-linking which can absorb a high volume of water molecule and swell without dissolving. Water absorbability of hydrogels is due to hydrophilic functional groups of the polymeric chain while resistance of these materials against dissolution in water is due to cross-linking among the network chains[1].
Capability of these intelligent agents to respond to various physical and chemical stimuli such as temperature [2-5], pH [6-8], mechanical load [9], light [10-13], electrical field [14] has attracted the interest of several researchers within the past years. Among other interesting properties of hydrogels, we may refer to biocompatibility property of these materials with human body and their large deformations. Hence, intelligent hydrogels are used in wound dressing and bandages[15], drug release system [16, 17], tissue engineering [18], and fabrication of actuators [19, 20]. Moreover, due to hydrogels adaptation in physiological activities, they have been implemented in nature-inspired [21] and biomimetic actuators [22] . It is necessary to provide a suitable model for intelligent hydrogels to predict their behavior; and this has been addressed by several researchers within the past years. For this purpose, hydrogels will be analyzed and their behavior will be examined using numerical tools after extracting basic governing equations of the hydrogels. We may refer to Hong's theory of coupled diffusion and large deformation in gels as a pioneering work in this field. Following that, Hong et al. [23] developed a subroutine to simulate the inhomogeneous equilibrium swelling of intelligent gels under mechanical load. Chester and Anand developed a structural model for temperature-sensitive hydrogels and implemented it through ABAQUS software [24]. In this regard, Cai and Suo developed an equilibrium model for intelligent temperature-sensitive

hydrogels (PNIPAM) which was in good conformity with experimental results [25]. After precise examination of the model developed by Cai and Suo, an instability was observed in the presented results. In this regard, Mazaheri et al. [26]. developed a stable and continuous model for temperature-sensitive hydrogels (PNIPAM) and utilized their model to solve several problems. As this model will be used in this paper, we will briefly explain it herein [26]. Mechanics of inhomogeneous large deformation of photo-thermal PNIPAM hydrogels was studied by Toh et al [10]. Also, Mazaheri et al developed a 3D constitutive model for photo-thermal PNIPAM hydrogels by considering copper chlorophyllin nanoparticle agents attached to the networks[12]. Moreover, there are also constitutive models developed for pH sensitive hydrogels used to solve applied issues to which the readers may be referred [6, 27-29]. Also, fracture in as a highly nonlinear phenomena in mechanical response of cross-linked hydrogel have investigated by Lei et al by presenting a mesoscopic network mechanics and they compared it with experiments to reproduce the fracture process in these material[30].

The capability to respond to environmental stimuli in the form of large deformations is regarded as an interesting property of hydrogels due to which they have many applications in manufacturing microscale instruments in microfluidic systems. In this regard, these materials are used as micro-valve in microfluidic systems to control flow rate. Most of the works carried out in this field are influenced by the activities of Beebe et al. [16]. Considering hydrogel shell on a rigid core in contact with fluid, they studied regulating the flow passing through the channel by the hydrogel shell. Following that, He et al. studied the pH sensitive hydrogel micro-valve [31]. Zhang et al. studied the behavior of a pH sensitive hydrogel micro-valve by considering the interaction between fluid and structure (FSI) [32]. In addition, Arbabi et al. studied the layout effect of several pH sensitive hydrogel micro-valves by considering FSI effects [33]. Moreover, Mazaheri et al. examined the behavior of a one-way micro-valve with an arrow-shaped geometry and studied the parameters affecting the micro-valve function [34]. Then, the behavior of the functionally graded pH-sensitive hydrogel micro-valve and temperature-sensitive micro-channel studied with different distribution of properties [35-38].

On the other hand, bending and self-folding properties of bilayer and multilayer hydrogel structures and twisting behavior of them with various sensitivities in contact with fluid in microscale has attracted the attention of researchers which has interesting applications especially in different applications [31, 39, 40]. Wu et al. studied the surface instability arising from swelling of hydrogel layers with variable properties along thickness [41]. Moreover, Abdolahi et al. dealt with analytical and numerical study of deformations of two-layer and three-layer micro-beam actuator of temperature-sensitive hydrogel with an elastomer sub-layer [20, 42]. After that, functionally graded and composite hydrogels in the form of temperature-sensitive micro-beams and micro-valves were addressed by some researchers [43, 44]. In addition to bending and self-folding responding, twisting properties is also among the responses of actuators[45] of which some of them design has been inspired in some cases from natural organs and special plants[46]. In this regard, Wang et al. studied bending and twisting deformations of plant tendril soft actuators in response to light radiation [47]. Jeong et al. studied the twisting, self-folding and bending mechanisms of 3D actuators converted from the planned 2D structures [48]. Moreover, Bayat et al. modeled and designed temperature/pH biphasic twisting hydrogel actuators. They also studied the effect of various layouts of elastomer and hydrogel as well as that of various parameters in the twisting function of biphasic actuator [49]. Huang et al. developed a numerical-experimental investigation on hydrogel-based bi-material beam structures in 2D self-scroll and 3D self-helical configurations by considering curvature and the mismatch

strain between material interfaces[50]. Furthermore, Hu et al. investigated behavior of different bilayer temperature-sensitive hydrogel-based actuators in several application such as: hydrogel grippers, self-folding box, origami driven and paper aeroplane model by presenting a modified free energy density for temperature-sensitive hydrogel[51].

In the present research, a three-layer twisting actuator made of temperature-sensitive hydrogel and elastomeric layer inspired from natural organs is studied numerically. Parametric studies are carried out on the mentioned actuator and the effects of geometric and material parameters neglecting the interface effects will be discussed to reach best performance of these actuators. This paper has been arranged as follows: At first, the proposed twisting actuator of this study will be described. Next, the constitutive models used for the temperature-sensitive hydrogel and the elastomer layers are presented. In the third section, simulation results and various conducted parametric studies will be dealt with. Finally, the results of this research are summarized in section 4.

2) Describing the twisting actuator and the material models

Figure 1 shows a schematic view of the 3D twisting actuator of this work that borrowed from the studies and tests conducted by Jeong et al. [48] at the reference temperature ($310K$). As it can be seen in the figure, the twisting actuator is considered constituting two temperature-sensitive hydrogel layers and one elastomeric layer. Volumetric percentage of both parts is the same and each one forms 50% of the actuator's volume in Figure 1. In this research, various volumetric percentages are considered for the structure of twisting actuator and the results arising from change of this parameter will be reviewed in the next sections. Another important point in examining the behavior of the 3D twisting actuator of this study, is the interface angle of hydrogel and elastomer layers which is shown by parameter α (Figure 1). This parameter has an important effect on the twisting behavior of the biphasic actuator that will be discussed in the next section. The length, width and depth of the initial biphasic twisting actuator are considered as $25mm$, $1.5mm$ and $80mm$, respectively (Figure 1). These dimensions and their corresponding effects arising from their changes will be completely reviewed in section 3. Moreover, elastomer stiffness has a high effect on twisting behavior of the actuator. Cross-linking density of the hydrogel which in fact indicates hydrogel stiffness is another parameter which will be studied. In this regard, a detailed study has been conducted on different values of cross-density of the hydrogel on twisting behavior of the actuator.

To clarify the simulations through this paper, we assign a code to each simulation as shown in eq.(1) that defines its geometric and material properties as *NxHy.yyAzz.zzVPww.ww*. In this notation, *x* indicates value of crosslinking density (Nv) multiplied by 100, *y.yy* shows the height of the cross-section (*H*), and *zz.zz* represnts the value of α in degrees, and *ww.ww* stands for volumertic percentages of the hydrogel . For instance, a twisting hydrogel actuator with crosslinking density of $Nv=0.03$, height of cross-section of *1.50*, angle of hydrogel and elastomer of *83.15°* with the hydrogel volume percentage of 50 % should be noted by *N3H1.50A83.15VP50.00.*

Simulations code: $\underbrace{Nx}_{\text{crosslinking density}\times 100}\ \overbrace{Hy.yy}^{\text{Height of the cross-section (H)}}\ \underbrace{Azz.zz}_{\text{value of }\alpha o}\ \overbrace{VPww.ww}^{\text{Hydrogel volumertic percentages}}$ (1)

In this paper, the model presented by Mazaheri et al. [26] is used to model the behavior of temperature-sensitive hydrogel part. In this model, modifications have been used to present numerical stability of the model near the phase transition temperature which is quite suitable to be implemented in FEM numerical tools. By considering coordinates of a

material point in reference and current states as X and $\mathbf{x}(\mathbf{X})$, deformation gradient tensor is defined as $\mathbf{F} = \partial\mathbf{x} / \partial\mathbf{X}$. Moreover, right Cauchy Green tensor is $\mathbf{C} = \mathbf{F}^T \mathbf{F}$. Using Lagrangian description, nominal stress components are derived from free energy density by differentiating with respect to $\mathbf{F}$. Assuming the low cross-linking density of hydrogel network, additive decomposition of the free energy density can be used for the hydrogels as follows which includes mechanical and mixing parts [52]:

$$W = W_{Stretch} + W_{Mixing} \tag{2}$$

where, $W_{Stretch}$ and W_{Mixing} are free energy density changes arising from mechanical deformations and mixing between hydrogel chains and water molecules, respectively. Due to the incompressibility of the hydrogel chains and water molecules, free energy is as follows [26]:

$$W = \frac{1}{2}NKT\left(I_1 - 3 - 2\log(J)\right) + \frac{k_B T}{\nu}(J-1)\left(-\frac{1}{J} - \frac{1}{2(J)^2} - \frac{1}{3(J)^3} + \frac{\chi(\phi,T)}{J}\right) \tag{3}$$

where, N is the density of the hydrogel chains, K is Boltzmann constant, T is the absolute temperature, $J = \det(\mathbf{F}) = 1 + \nu C = 1/\phi$ is deformation gradient determinant, I_1 is the first invariant $\mathbf{C}$, and ν is solvent molecule volume. Moreover, χ is mixing parameter between water and PNIPAM temperature-sensitive hydrogel presented by Afroze et al. [53] as $\chi = A_0 + B_0 T + (A_1 + B_1 T)\phi$. Based on their experiments they obtained the material constants as $A_0 = -12.947$, $B_0 = 0.04496K^{-1}$, $A_1 = 17.92$ and $B_1 = -0.0569K^{-1}$.

As it was said earlier, a suitable subroutine has been developed to use this model in solving finite elements problems in ABAQUS. On the other hand, since an initial reference temperature has been defined for the actuator with a stress-free state, the expression related to free energy shall be rewritten with an initial stretch of λ_0 relative to the initial reference temperature.

The elastomeric part of twisting actuator subject of this study is incompressible and is regarded as a hyperelastic material for which free energy is stated based on Neo-Hookean theory as follows [20]:

$$W_{Elastomer} = \frac{1}{2}G\left(I_1 - 3 - 2\log(J)\right) + \pi(\ln(J))^2 \tag{4}$$

where, G is the elastic shearing module of the elastomer and π is the Lagrangian coefficient indicating the hydrostatic pressure arising from incompressibility of the elastomer. The simulations in this paper were made in a temperature range of $302 - 310K$ including phase transition interval of the hydrogel. At the reference temperature of $310K$, the twisting actuator is in free-stress state and it twists with the decrease in temperature and swelling of hydrogel due to structural asymmetry of the actuator which will be discussed in the next section.

3) Results and discussion

In this section, the behavior of biphasic twisting actuator is studied in a temperature range of 302-310 K. As the temperature decreases from $310K$ to $302K$, the hydrogel section swells and the actuator twists due to the difference between the elastomer and the hydrogel properties. For numerical studies, a twisting actuator is first examined which is fixed in one end and is free to twist in other one. The effects of various parameters, such as interface angle α, hydrogel cross-linking density *(Nν)*, cross-section dimensions and the hydrogel volumetric percentage, on the behavior of the twisting actuator are

considered in the following. For each parameter, its optimum value is specified for which the maximum twisting angle is obtained. Then, in order to examine the actuator's capability to produce reaction torque against possible obstacle, the under-study actuator is constrained at both two ends to prevent it from twisting. As the temperature decreases, the actuator tends to be twisted and, as a result, a torsional reaction torque is developed in the actuator. In this situation, the torsional torque developed in the bearings is calculated to reach a judgement about the actuator capability to produce torsional torque.

At first, hydrogel and elastomer volumes are considered fixed in all cases. 50% of actuator's volume is comprised of hydrogel and the other 50% comprises elastomer. In this study, a linear hexagonal element (C3D8H) is used to model the twisting actuator. Mesh study has been conducted separately to find the optimum mesh size. Twisting angle of actuator is obtained based on temperature changes and is shown in Figure 2. To study the mesh size effect, meshes with different sizes of 4, 3, 2, 1 and 0.85 were studied in an actuator with *N3H1.50A83.15VP50.00*. As seen in the Figure 2, twisting angle increases with the decrease of elements size. Finally, the results conform to each other for mesh sizes of 0.85 and 1. As a result, the mesh with the size of 0.85 is selected for simulations of this work.

3.1) Twisting angle of the actuator

In this section, we study deformation of the twisting actuator with a fixed end while the other end is free to move. As temperature decreases from $310K$ to $302K$, the hydrogel section swells and the actuator twists. Simulation results of twisting actuator for hydrogel volume percentage of 50% at different temperatures is shown in Figure 3. As seen in Figure 3-a, the actuator is in stress-free state in a reference temperature of $310K$. As temperature decreases, hydrogel starts swelling and twisting around the longitudinal axis of the actuator (z axis). Twisting of the actuator as a result of the hydrogel swelling continues to $302K$. As it is seen in the figure, the highest twisting of the actuator occurs in $302K$ at the free end of actuator (Figure 3-e). Effects of various parameters on the twisting behavior of the under-study actuator will be studied in the next section.

3.1.1) Effects of Nv ***and*** α

One of the parameters that affects the actuator's behavior is the stiffness of hydrogel which is directly associated with its cross-linking density (Nv). As the density of cross-linking in hydrogel increases, hydrogel becomes more rigid and shows a higher resistance against deformation due to temperature decrease. Hence, the amount of twisting angle is expected to decrease by the increase in Nv. On the other hand, angle α between the hydrogel and elastomer layers severely affects the actuator's performance. Therefore, changes in twisting angle for an actuator with dimensions of *H1.50* is studied for 8 different angles of α and 3 different values of Nv due to temperature changes and the results are given in Figure 4.

As expected, twisting angle of the actuator decreases by increase in Nv. Moreover, it can be seen in Figure 4-a that when $\alpha = 83.15^{\circ}$, we have the least twisting angle. This may be due to difference in connection of layers among this case and other cases; because in this case, the interface between hydrogel and elastomeric layers passes through the corner of cross-section of the actuator. This is while in other states, interface collides only with one edge of the cross-section. In addition, all curves show a sharp change in the temperature range of $305-308K$ which is due to phase transition of hydrogel and spurt swelling in this temperature range.

To understand the simultaneous effect of temperature and angle α, 3D plots for the change of twisting angle are given versus both the temperature and the angle α for different Nvs in Figure 5. It is clear that actuator's twisting angle in $Nv = 0.03$ is more

sensitive to angle α changes compared to others. Existence of optimum value for α to have the maximum twisting angle can be seen in these diagrams.
Since the most changes in the twisting angle is observed for $Nv = 0.03$, this value is considered for all other simulations of this work to obtain more details about the effect of other parameters on twisting behavior of the actuator. In the following, the twisting angle of the actuator is obtained for different values of the angle α from $\alpha = 83.15^\circ$ to $\alpha = 65^\circ$ as shown in Figure 6 for $Nv = 0.03$.
As illustrated in Figure 6, the least twisting angle occurs in $\alpha = 83.15^\circ$. On the other hand, twisting angle increases by the decreasing α from 83.15° to 75°. Then, twisting angle decreases by decrease of angle α from 75° to 65° which indicates the effect of angle α on twisting behavior of the actuator and it clearly confirms existence of an optimal value for α with the maximum twisting angle.

3.1.2) Effect of the actuator cross-section dimensions

Dimensions of the actuator's cross-section is another parameter which has a significant impact on the actuator's twisting behavior. In this section, the behavior of twisting actuator with different cross-section dimensions is numerically studied and the results are shown in Figure 7. It should be noted that in these simulations, the amount of the cross-section area and the volume ratio of the hydrogel and the elastomer remains unchanged. Moreover, the effect of angle α is studied for each of the dimensions of under-study actuator, while the length of twisting actuator is considered constant. Considering the remarks of the previous section, all simulations are considered with cross-linking density of $Nv = 0.03$. As shown in Figure 7, the maximum twisting angle is obtained for *H2.50* when *H* varies from 1.50 to 3.00. Thus, in the following we conduct the remaining parameter studies for *H2.50*.
Dimensional examinations indicate that the highest twisting angle occurs for the case with the dimension of *H2.50* (Figure 7-c). Such a large twisting angle is considerably different from the initial case with dimension of *H1.50* (Figure 7-a). Moreover, in this model, the angle $\alpha = 35^\circ$ is the angle in which the twisting actuator experiences the highest level of twist. As the length and width of cross-section approaches each other, temperature range in which sudden changes of twisting angle occurs, gets close to $306K$. It should be noted that upon decrease of angle α from 35°, the difference between twisting angles decreases to the extent where such differences can be ignored. As illustrated in Figure 7, for all cases the maximum of the twisting angle is obtained for one with the interface line does not pass through the corners of the cross-section. Thus, generally we can conclude that to reach the maximum twisting angle we should select the geometry that interface line does not pass through the corners of the actuator.

3.1.3) Study of the volumetric percentage of hydrogel effect on the twisting actuator

In the previous section, it was specified that the highest twisting angle occurs in an actuator with the dimension of *H2.50*. In all cases examined so far, volumetric percentages of hydrogel and elastomer were equal to 50%. Now in this section, the impacts arising from the change in volumetric percentages of the hydrogel and the elastomer on the twisting behavior of the actuator is studied. A model with dimensions of *H2.50* and *A50.00* is used for this purpose that as shown in the previous section, has the largest twisting angle in comparison with the other cross-section dimensions. For the better understanding about the volumetric percentage of the hydrogel in the actuator, Figure 8 is provided that includes schematics of actuators with 4 different values of the volumetric percentage of the hydrogel. Also, numerical results of these actuators are illustrated in Figure 9. For an optimal study, all cases are modeled in this section with

$\alpha = 35^\circ$ which is the angle with the highest twisting angle for *H2.50* as shown in the previous section. Figure 10 and Figure 11 show the effects of the various volumetric percentages of the hydrogel on the twisting angle of the actuator versus temperatures changes.

The case with lower values of *VP* (lower contents of hydrogel) needs larger swelling of the hydrogel for twisting that needs more decrease in the temperature from the reference temperature of $310K$. Thus, as illustrated in Figure 10, the temperature at which the actuator starts to twist decreases from $308K$ to $306K$ as *VP* decreases from 60% to 45%. But, to reach the maximum twisting angle we have an optimal value for the value of *VP*. Considering Figure 10, the maximum amount of twisting angle which is of around 625.42°, occurs when 50% of the actuator is comprised of hydrogel. As a result, the case with *N3H2.50A35.00VP50.00* is recognized the best option for the actuator with maximum twisting angle.

3.2) Reaction torque of the actuator

The studies conducted in the previous sections were all pertinent to twisting actuators with one free end and one fixed end. Here, to study the capability of the actuator in torsional torque generation at the time of collision with an obstacle, the under-study actuator with one fixed end and one without rotation is investigated and the reaction torque of the bearings is calculated. In this section, first the initial model of twisting actuator with the dimension of *H1.50* and $\alpha = 83.15^\circ$ is analyzed which was formerly depicted in Figure 1 and the obtained results are shown in Figure 11.

As seen in Figure 11, two ends of the actuator have no rotation but due to swelling of the hydrogel and tendency of the actuator to twisting, other sections of the actuator experience twisting that is anti-symmetric with respect to its mid-plane in axial direction. The maximum twisting angle occurs in the middle of the actuator because it has the farthest distance from the constrained ends of the twisting actuator. It should be noted that similar to the previous section, the reaction torque depend on some variables and parameters such as temperature changes, cross-linking density of Nv, angle α, cross-section dimensions and volumetric percentage of the hydrogel. First, the effects of the cross-linking density Nv, as well as the effect of the angle α, are studied and the obtained results are shown in Figure 12.

In Figure 12, it can be seen that by decreasing the temperature form the reference temperature of $310K$, the reaction torque increases due to swelling of the hydrogel and tendency of the actuator to twist. But, as stems from all curves, after 1-2 K decrease in temperature, the reaction torque encounters a sharp decrease that is because of the instability of the actuator after swelling of the hydrogel and buckling of the deformed structure. Thus, the user of theses actuators should be aware about this phenomenon and prevent the actuator from that temperature ranges in which this instability occurs. Also, for the angles of $\alpha = 65^\circ$ and $\alpha = 75^\circ$ in all Nvs, the maximum reaction torque is smaller than the case with $\alpha = 83.15^\circ$. As mentioned before, it can be due to difference in connection points of layers in cross-section of the actuator so that the interface of layers crosses the corners of the cross-section when $\alpha = 83.15^\circ$. Thus, in the following only $\alpha = 83.15^\circ$ will be considered for the remaining study of the Nv effect. The effect of cross-linking density (Nv), is illustrated in Figure 13. As expected, the maximum reaction torque is obtained for the maximum value of Nv due to the larger stiffness of the hydrogel layer that results in producing larger amounts of reactions. In the following (Figure 14), the effects of angle α as well as size of the actuator on the reaction torque are investigated for different cross-sections and the results are presented in Figure 13 and Figure 14.

According to Figure 14, it is seen that like Figure 12, in this case where the interface of hydrogel and elastomeric layers passes through the corners of the actuator, the amount of reaction torque is higher than other cases where the interface line doesn't pass through the corners of the actuator. Also, the amount of reaction torque decreases by the decrease of angle α and increase of interface distance from the corner of the actuator. In the following, the reaction torque of the cases with different cross-sections for which the interface passes through the corner of actuator are compared to find the maximum reaction torque (Figure 15).

Similar to other parameter studies, we assume a constant cross-section area for all analysis. The results indicate that the maximum reaction torque is obtained for the dimension of *H2.50*. In the following, the reaction torque is calculated for the actuator dimension of *H2.50* (i.e., an actuator with the maximum reaction torque), and the hydrogel volumetric percentage effect on the reaction torque is studied as depicted in Figure 16.

According to Figure 16, the amount of the reaction torque decreases by the increase of hydrogel volumetric percentage, and the highest torsional reaction torque occurs when 50% of the actuator is comprised of the hydrogel. As depicted in this figure, the case with *VP50.00* has the maximum torsional rigidity (maximum slope of the curve) as well as maximum reaction torque against the temperature changes. This case encounters the instability at the higher temperatures in comparison with the cases with *VP32.50* and *VP25.00* with the approximately the same reaction force. This is the cause of selection of *VP50.00* for the actuator with maximum resistance against the exterior loadings.

4) Summary and conclusion

In this paper, a twisting actuator comprised of temperature-sensitive PNIPAM hydrogel and elastomeric parts was studied. To simulate the twisting actuator, hydrogel behavior was first simulated in ABAQUS software by using UHYPER subroutine. The actuator was modeled and its twisting behavior was simulated due to the temperature decrease from $310K$ to $302K$. First, twisting angle of the actuator was investigated for a biphasic actuator with one fixed and one free ends, and the effect of different parameters such as interface angle (α), cross-linking density of the hydrogel (Nv), volumetric percentage of the hydrogel, and cross-section dimensions, on the behavior of twisting actuator were studied. According to the conducted studies, it was specified that twisting angle of the actuator was decreased by the increase of Nv. Moreover, upon change of angle α, twisting angle of the actuator has an optimum value for a specified actuator. Similar results were obtained for dimensions of cross-section of the actuator. The results indicated that an actuator with *N3H2.50A35.00VP50.00* had the maximum twisting angle. Following that, the reaction torque of the actuator was obtained for the case with two constrained ends. First, the cross-section dimension's effect as well as the hydrogel cross-linking density were investigated and the case with maximum reaction torque was selected. Then for the selected case, parametric studies showed that the maximum reaction torque occurred for the case with *N3H2.50A71.56VP50.00*.

As can be seen, the maximum twisting angle and reaction torque occurred for the case with *N3H2.50Azz.zzVP50*.00 for *A35.00* and *A71.56*, respectively. Thus, we concluded that for maximum twisting angle, the interface line should not pass through the actuator corners, while the maximum reaction torque occurred for case that interface line crossed the actuator corners.

Nomenclature

α	The interface angle of hydrogel and elastomer layers
H	The height of the cross-section
$W_{Stretch}$	Free energy density changes arising from mechanical deformations
W_{Mixing}	Free energy density changes arising from mixing between hydrogel chains and water molecules
$W_{Elastomer}$	Free energy density changes for incompressible elastomer
N	Density of the hydrogel chains
K	Boltzmann constant
T	The absolute temperature
$\mathbf{F} = \partial \mathbf{x} / \partial \mathbf{X}$	Deformation gradient
$J = \det(\mathbf{F})$	Deformation gradient determinant
$\mathbf{C} = \mathbf{F}^T \mathbf{F}$	Right Cauchy Green tensor
I_1	The first invariant $\mathbf{C}$
v	Solvent molecule volume
χ	Dimensionless mixing parameter
A_0, B_0, A_1, B_1	The material constants

References

1. Morkhande, V., Pentewar, R., Gapat, S., et al. "*A review on hydrogel", Indo American Journal of Pharmaceutical Research*, **6**(3), pp. 4678-4688 (2016).
2. Morimoto, T. and Ashida, F. "*Temperature-responsive bending of a bilayer gel", International Journal of Solids and Structures*, **56**, pp. 20-28 (2015).
3. Suzuki, A., Yoshikawa, S., and Bai, G. "*Shrinking pattern and phase transition velocity of poly (N-isopropylacrylamide) gel", The Journal of chemical physics*, **111**(1), pp. 360-367 (1999).
4. Shojaeifard, M. and Baghani, M. "*Finite deformation swelling of a temperature-sensitive hydrogel cylinder under combined extension-torsion", Applied Mathematics and Mechanics*, **41**(3), pp. 409-424 (2020).
5. Ghasemkhani, A. and Mazaheri, H. "*Study of Functionally Graded Temperature-Sensitive Hydrogel Micro-Valve Considering Fluid-Structure Interactions", Modares Mechanical Engineering*, **20**(4), pp. 943-951 (2020).
6. Marcombe, R., Cai, S., Hong, W., et al. "*A theory of constrained swelling of a pH-sensitive hydrogel", Soft Matter*, **6**(4), pp. 784-793 (2010).
7. Arbabi, N., Baghani, M., Abdolahi, J., et al. "*Finite bending of bilayer pH-responsive hydrogels: A novel analytic method and finite element analysis", Composites Part B: Engineering*, **110**, pp. 116-123 (2017).
8. Shojaeifard, M., Bayat, M., and Baghani, M. "*Swelling-induced finite bending of functionally graded pH-responsive hydrogels: a semi-analytical method", Applied Mathematics and Mechanics*, **40**(5), pp. 679-694 (2019).
9. Chester, S.A. and Anand, L. "*A coupled theory of fluid permeation and large deformations for elastomeric materials", Journal of the Mechanics and Physics of Solids*, **58**(11), pp. 1879-1906 (2010).
10. Toh, W., Ng, T.Y., Hu, J., et al. "*Mechanics of inhomogeneous large deformation of photo-thermal sensitive hydrogels", International Journal of Solids and Structures*, **51**(25-26), pp. 4440-4451 (2014).
11. Miar, S., Perez, C.A., Ong, J.L., et al. "*Polyvinyl alcohol-poly acrylic acid bilayer oral drug delivery systems: A comparison between thin films and inverse double network bilayers", Journal of biomaterials applications*, **34**(4), pp. 523-532 (2019).
12. Mazaheri, H., Namdar, A.H., and Ghasemkhani, A. "*A model for inhomogeneous large deformation of photo-thermal sensitive hydrogels", Acta Mechanica*, pp. 1-18 (2021).

13. Mazaheri, H., Ghasemkhani, A., and Namdar, A. "*Behavior of photo-thermal sensitive polyelectrolyte hydrogel micro-valve: analytical and numerical approaches", Journal of Stress Analysis*, **5**(1), pp. 21-30 (2020).
14. Li, H. "*Kinetics of smart hydrogels responding to electric field: A transient deformation analysis", International Journal of Solids and Structures*, **46**(6), pp. 1326-1333 (2009).
15. Hu, J., Wei, T., Zhao, H., et al. "*Mechanically active adhesive and immune regulative dressings for wound closure", Matter*, **4**(9), pp. 2985-3000 (2021).
16. Beebe, D.J., Moore, J.S., Bauer, J.M., et al. "*Functional hydrogel structures for autonomous flow control inside microfluidic channels", Nature*, **404**(6778), pp. 588-590 (2000).
17. Eddington, D.T. and Beebe, D.J. "*Flow control with hydrogels", Advanced drug delivery reviews*, **56**(2), pp. 199-210 (2004).
18. Ahadian, S., Sadeghian, R.B., Yaginuma, S., et al. "*Hydrogels containing metallic glass sub-micron wires for regulating skeletal muscle cell behaviour", Biomaterials science*, **3**(11), pp. 1449-1458 (2015).
19. Xia, C., Lee, H., and Fang, N. "*Solvent-driven polymeric micro beam device", Journal of Micromechanics and Microengineering*, **20**(8), pp. 085030 (2010).
20. Abdolahi, J., Baghani, M., Arbabi, N., et al. "*Analytical and numerical analysis of swelling-induced large bending of thermally-activated hydrogel bilayers", International Journal of Solids and Structures*, **99**, pp. 1-11 (2016).
21. Li, W., Guan, Q., Li, M., et al. "*Nature-inspired strategies for the synthesis of hydrogel actuators and their applications", Progress in Polymer Science*, **140** (2023).
22. Huang, Y.-C., Cheng, Q.-P., Jeng, U.-S., et al. "*A Biomimetic Bilayer Hydrogel Actuator Based on Thermoresponsive Gelatin Methacryloyl–Poly (N-isopropylacrylamide) Hydrogel with Three-Dimensional Printability", ACS Applied Materials & Interfaces*, (2023).
23. Hong, W., Liu, Z., and Suo, Z. "*Inhomogeneous swelling of a gel in equilibrium with a solvent and mechanical load", International Journal of Solids and Structures*, **46**(17), pp. 3282-3289 (2009).
24. Chester, S.A. and Anand, L. "*A thermo-mechanically coupled theory for fluid permeation in elastomeric materials: application to thermally responsive gels", Journal of the Mechanics and Physics of Solids*, **59**(10), pp. 1978-2006 (2011).
25. Cai, S. and Suo, Z. "*Mechanics and chemical thermodynamics of phase transition in temperature-sensitive hydrogels", Journal of the Mechanics and Physics of Solids*, **59**(11), pp. 2259-2278 (2011).
26. Mazaheri, H., Baghani, M., Naghdabadi, R., et al. "*Inhomogeneous swelling behavior of temperature sensitive PNIPAM hydrogels in micro-valves: analytical and numerical study", Smart Materials and Structures*, **24**(4), pp. 045004 (2015).
27. Lee, Y.J. and Braun, P.V. "*Tunable inverse opal hydrogel pH sensors", Advanced Materials*, **15**(7- 8), pp. 563-566 (2003).
28. He, T., Li, M., and Zhou, J. "*Modeling deformation and contacts of pH sensitive hydrogels for microfluidic flow control", Soft Matter*, **8**(11), pp. 3083-3089 (2012).
29. Drozdov, A. and Christiansen, J.d. "*Time-dependent response of hydrogels under multiaxial deformation accompanied by swelling", Acta Mechanica*, **229**(12), pp. 5067-5092 (2018).
30. Lei, J., Li, Z., Xu, S., et al. "*A mesoscopic network mechanics method to reproduce the large deformation and fracture process of cross-linked elastomers", Journal of the Mechanics and Physics of Solids*, **156**, pp. 104599 (2021).
31. He, H., Guan, J., and Lee, J.L. "*An oral delivery device based on self-folding hydrogels", Journal of controlled release*, **110**(2), pp. 339-346 (2006).
32. Zhang, Y., Liu, Z., Swaddiwudhipong, S., et al. "*pH-sensitive hydrogel for micro-fluidic valve", Journal of functional biomaterials*, **3**(3), pp. 464-479 (2012).
33. Arbabi, N., Baghani, M., Abdolahi, J., et al. "*Study on pH-sensitive hydrogel micro-valves: A fluid–structure interaction approach", Journal of Intelligent Material Systems and Structures*, **28**(12), pp. 1589-1602 (2017).

34. Mazaheri, H., Namdar, A., and Amiri, A. "*Behavior of a smart one-way micro-valve considering fluid–structure interaction", Journal of Intelligent Material Systems and Structures*, **29**(20), pp. 3960-3971 (2018).
35. Mazaheri, H., Ghasemkhani, A., and Sabbaghi, S. "*Study of Fluid-Structure Interaction in a Functionally Graded Ph-Sensitive Hydrogel Micro-Valve", International Journal of Applied Mechanics*, (2020).
36. Ghasemkhani, A., Mazaheri, H., and Amiri, A. "*Fluid-structure interaction simulations for a temperature-sensitive functionally graded hydrogel-based micro-channel", Journal of Intelligent Material Systems and Structures*, pp. 1045389X20963170 (2020).
37. Mazaheri, H. and Khodabandehloo, A. "*Behavior of an FG temperature-responsive hydrogel bilayer: Analytical and numerical approaches", Composite Structures*, **301**, pp. 116203 (2022).
38. Khodabandehloo, A. and Mazaheri, H. "*Analytic and finite element studies on deformation of bilayers with a functionally graded pH-responsive hydrogel layer", International Journal of Applied Mechanics*, **14**(5), pp. 2250053 (2022).
39. Randall, C.L., Gultepe, E., and Gracias, D.H. "*Self-folding devices and materials for biomedical applications", Trends in biotechnology*, **30**(3), pp. 138-146 (2012).
40. Xiang, S.-L., Su, Y.-X., Yin, H., et al. "*Visible-light-driven isotropic hydrogels as anisotropic underwater actuators", Nano Energy*, **85**, pp. 105965 (2021).
41. Wu, Z., Bouklas, N., and Huang, R. "*Swell-induced surface instability of hydrogel layers with material properties varying in thickness direction", International Journal of Solids and Structures*, **50**(3-4), pp. 578-587 (2013).
42. Abdolahi, J., Baghani, M., Arbabi, N., et al. "*Finite bending of a temperature-sensitive hydrogel tri-layer: An analytical and finite element analysis", Composite Structures*, **164**, pp. 219-228 (2017).
43. Shojaeifard, M., Rouhani, F., and Baghani, M. "*A combined analytical–numerical analysis on multidirectional finite bending of functionally graded temperature-sensitive hydrogels", Journal of Intelligent Material Systems and Structures*, **30**(13), pp. 1882-1895 (2019).
44. Mazaheri, H. and Ghasemkhani, A. "*Analytical and Numerical Study of the Swelling Behavior in Functionally Graded Temperature-sensitive Hydrogel Shell", Journal of Stress Analysis*, **3**(2), pp. 29-35 (2019).
45. Chen, F., Miao, Y., Gu, G., et al. "*Soft Twisting Pneumatic Actuators Enabled by Freeform Surface Design", IEEE Robotics and Automation Letters*, **6**(3), pp. 5253-5260 (2021).
46. Zou, M., Li, S., Hu, X., et al. "*Progresses in Tensile, Torsional, and Multifunctional Soft Actuators", Advanced Functional Materials*, pp. 2007437 (2021).
47. Wang, M., Lin, B.-P., and Yang, H. "*A plant tendril mimic soft actuator with phototunable bending and chiral twisting motion modes", Nature communications*, **7**(1), pp. 1-8 (2016).
48. Jeong, K.-U., Jang, J.-H., Kim, D.-Y., et al. "*Three-dimensional actuators transformed from the programmed two-dimensional structures via bending, twisting and folding mechanisms", Journal of Materials Chemistry*, **21**(19), pp. 6824-6830 (2011).
49. Bayat, M. and Baghani, M. "*Finite element modeling and design of pH/temperature sensitive hydrogel based biphasic twisting actuators", scientiairanica*, **26**(4), pp. 2356-2368 (2019).
50. Huang, R., Xue, Y., Li, Z., et al. "*Programmable Spiral and Helical Deformation Behaviors of Hydrogel-Based Bi-Material Beam Structures", International Journal of Structural Stability and Dynamics*, **20**(13), pp. 2041010 (2020).
51. Hu, J., Jiang, N., and Du, J. "*Thermally controlled large deformation in temperature-sensitive hydrogels bilayers", International Journal of Smart and Nano Materials*, **12**(4), pp. 450-471 (2021).
52. Hong, W., Zhao, X., Zhou, J., et al. "*A theory of coupled diffusion and large deformation in polymeric gels", Journal of the Mechanics and Physics of Solids*, **56**(5), pp. 1779-1793 (2008).

53. Afroze, F., Nies, E., and Berghmans, H. "*Phase transitions in the system poly (N-isopropylacrylamide)/water and swelling behaviour of the corresponding networks*", *Journal of Molecular Structure*, **554**(1), pp. 55-68 (2000).

Figures:

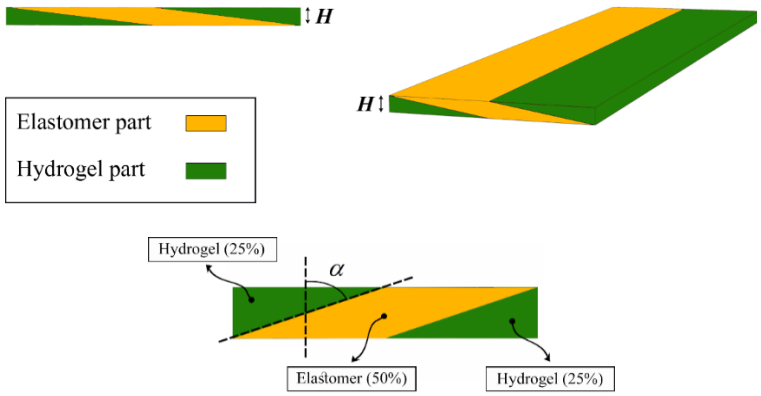

Figure 1. Schematics of the biphasic twisting actuator and angle α

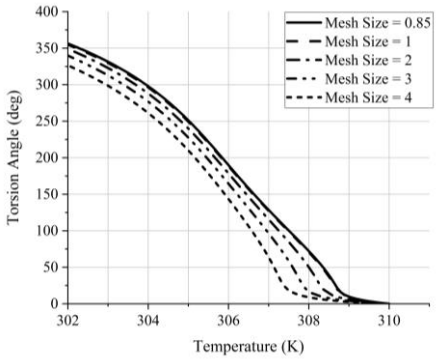

Figure 2. An example for the mesh study of the twisting actuator with *N3H1.50A83.15VP50.00.*

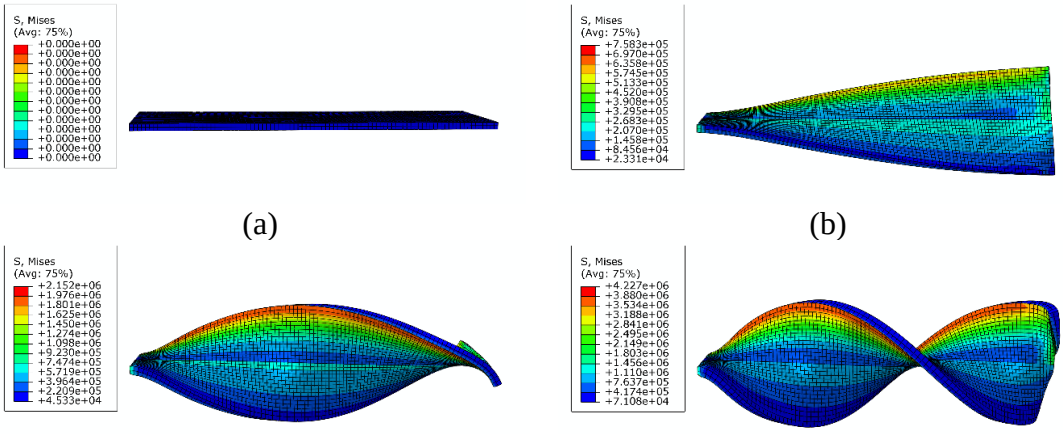

(c) (d)

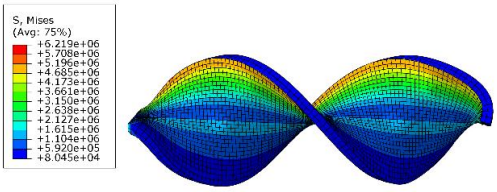

(e)

Figure 3. Deformation of the actuator with *N3H1.50A83.15VP50.00* at the temperature of (a) $310K$, (b) $308K$, (c) $306K$, (d) $304K$, and (e) $302K$.

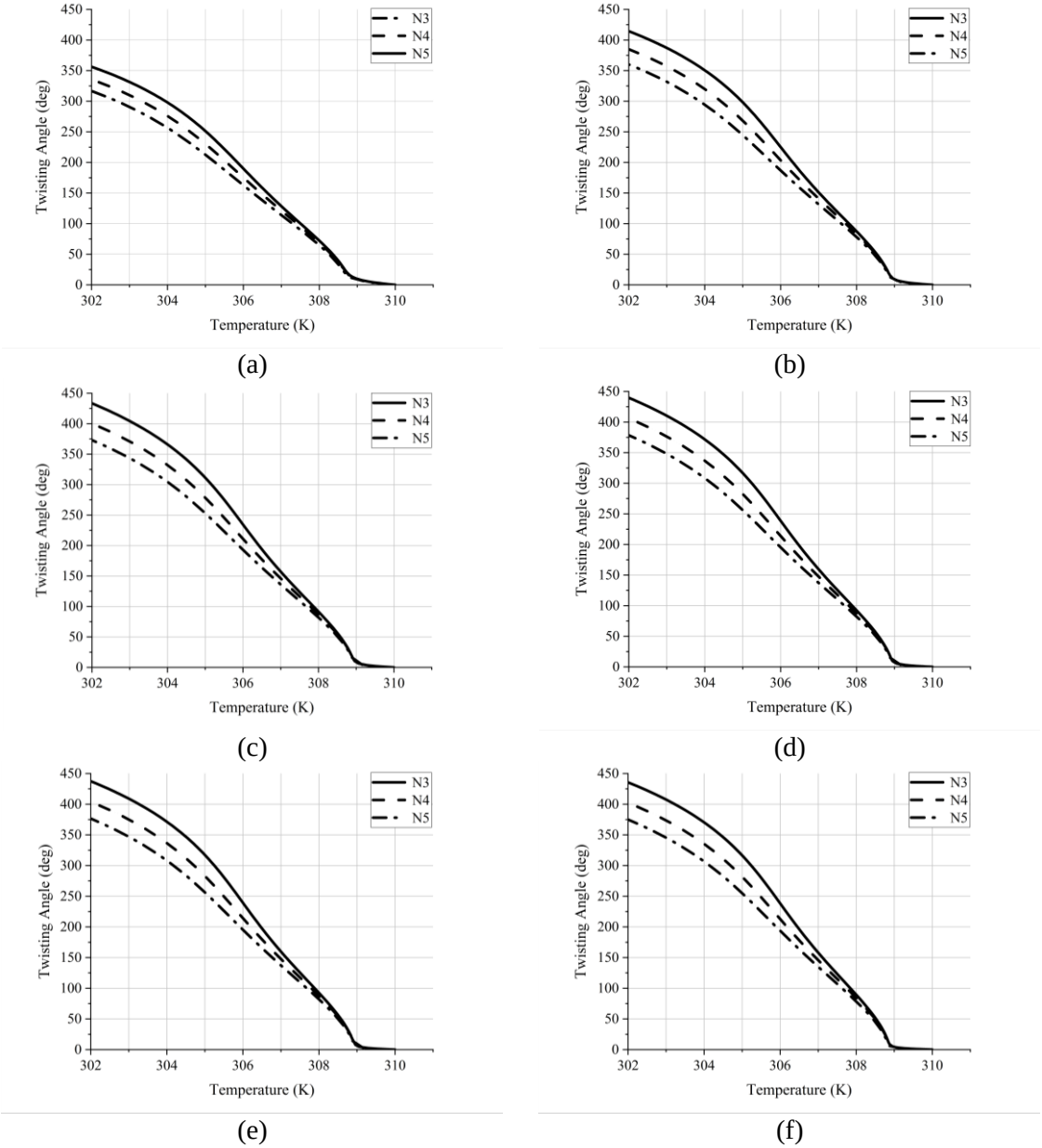

(a) (b)

(c) (d)

(e) (f)

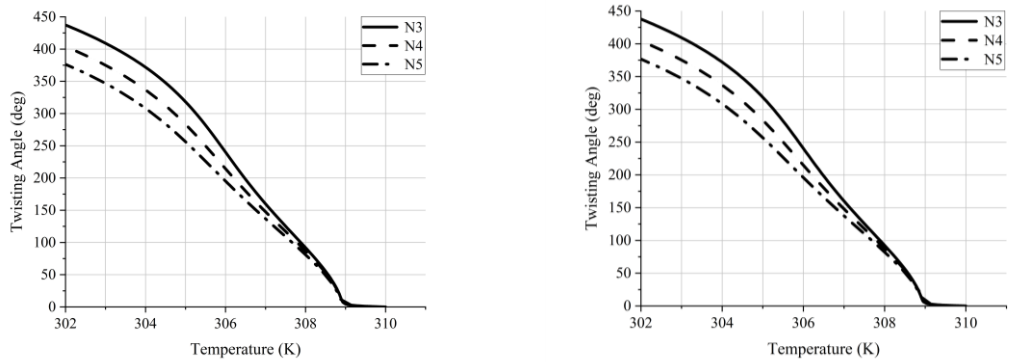

(g) (h)

Figure 4. Variations of twisting angle of the actuator with *NxH1.50Azz.zzVP50.00* due to temperature changes for (a) *A83.15*, (b) *A80.00*, (c) *A77.50*, (d) *A75.00*, (e) *A72.50*, (f) *A70.00*, (g) *A67.50*, and (h) *A65.00*

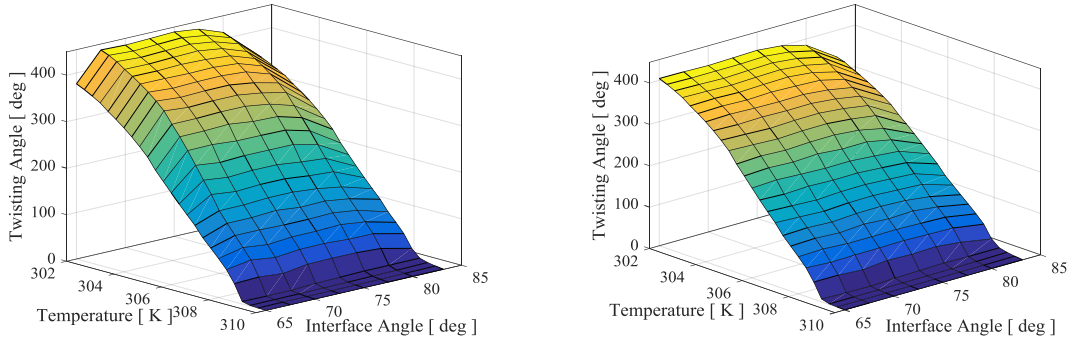

(a) (b)

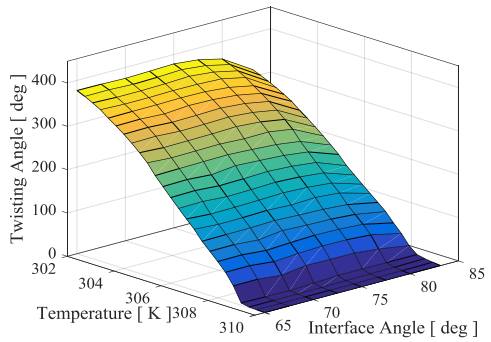

(c)

Figure 5. 3D chart for twisting angle of the actuator with *NxH1.50Azz.zzVP50.00* in terms of temperature changes for (a) *N3*, (b) *N4*, and (c) *N5*.

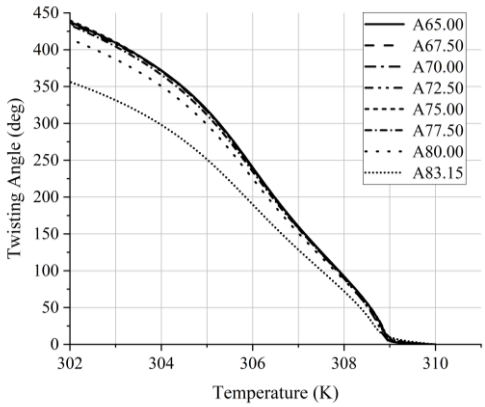

Figure 6. simulation results for twisting angle of the actuator with *N3H1.50Azz.zzVP50.00* in terms of the temperature changes.

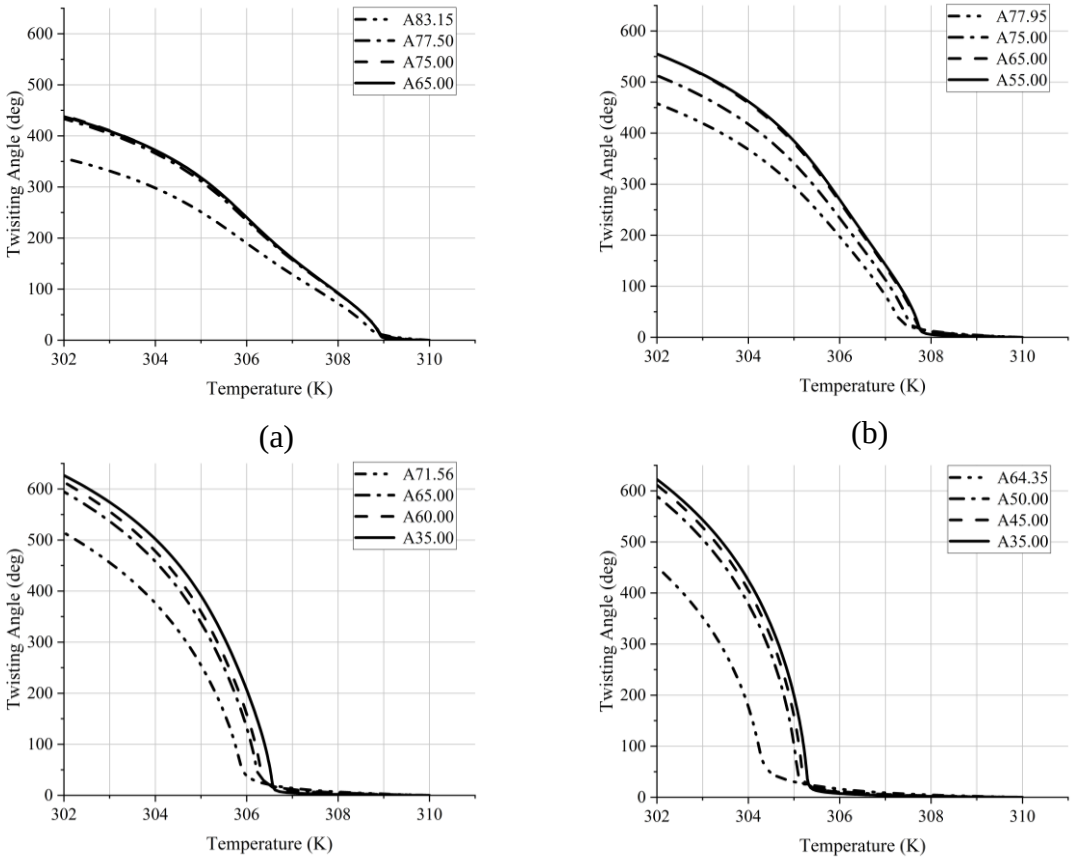

Figure 7. Twisting angles of the under-study actuator with *N3Hy.yyAzz.zzVP50.00* for (a) *H1.50*, (b) *H2.00*, (c) *H2.50*, and (d) *H3.00*.

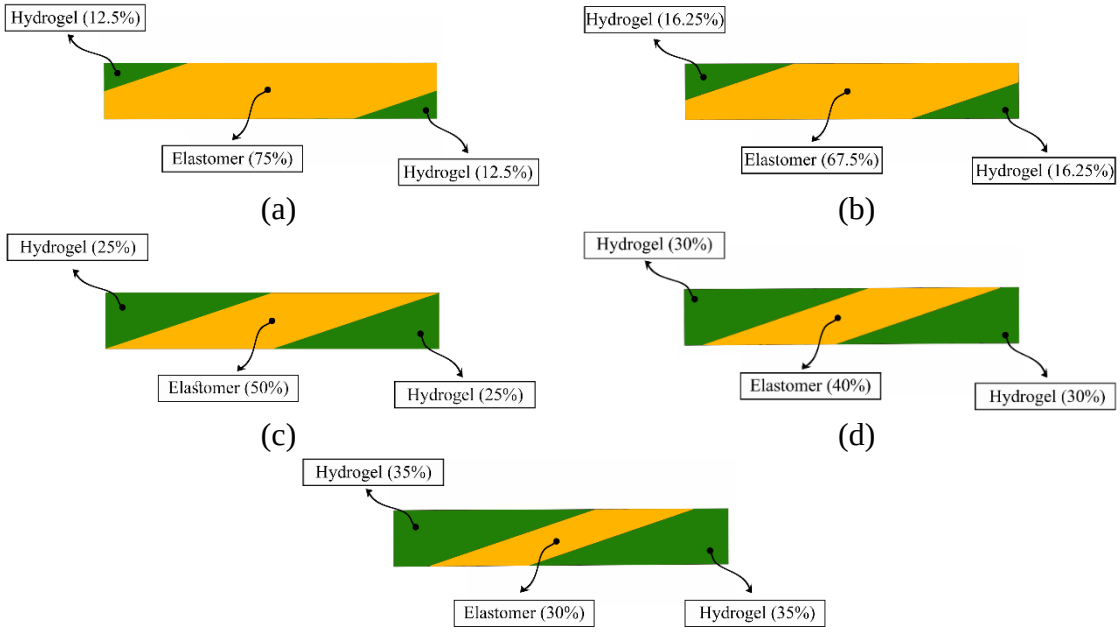

Figure 8. Different actuators with *N3Hy.yyA35.00VPww.ww* for (a) *VP25.00*, (b) *VP32.50*, (c) *VP60.00*, and (d) *VP70.00*

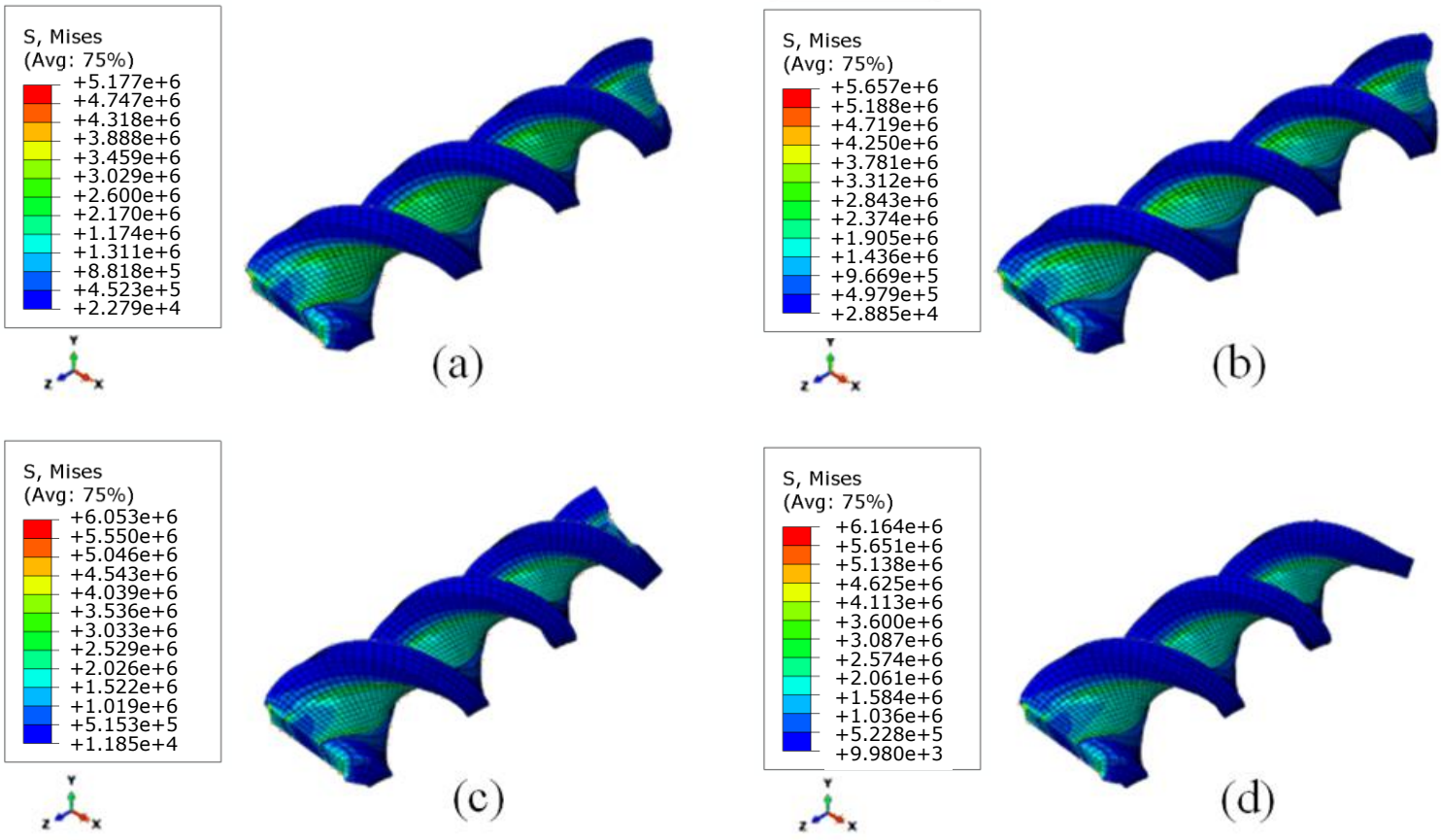

Figure 9. Twisting of an actuator with *N3H2.50A35.00VPww.ww* for (a) *VP45.00*, (b) *VP50.00*, (c) *VP55.00*, and (d) *VP60.00* at temperature of $302K$.

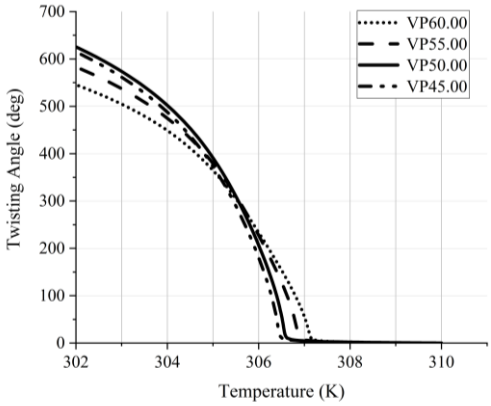

Figure 10. Effects of volumetric percentage of the hydrogel on the twisting angle of an actuator with *N3H2.50A35.00VPww.ww*

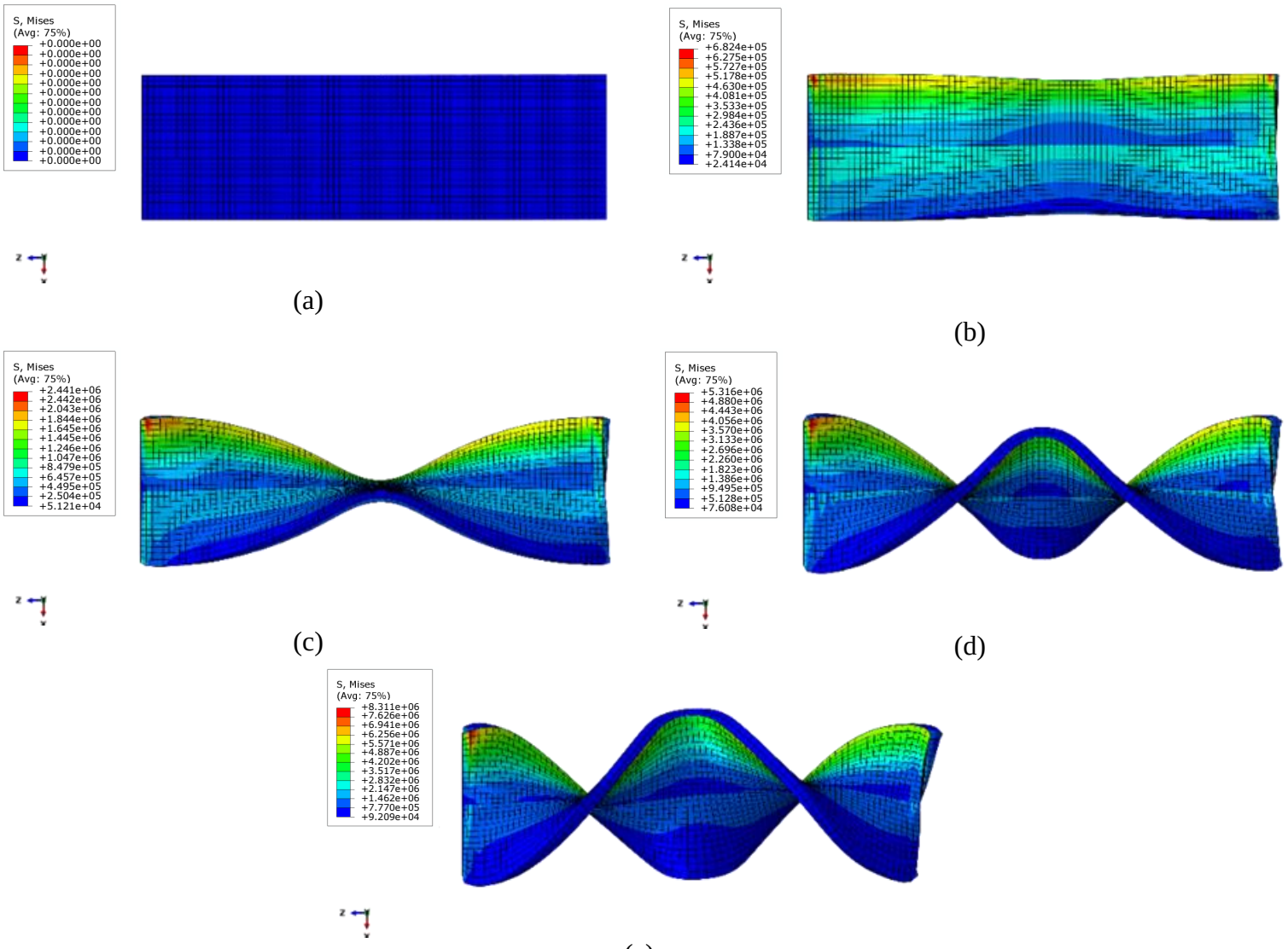

Figure 11. Simulation results for the actuator with *N3H1.50A83.15VP50.00* and with two constrained ends at (a) $310K$, (b) $308K$, (c) $306K$, (d) $304K$, and (e) $302K$.

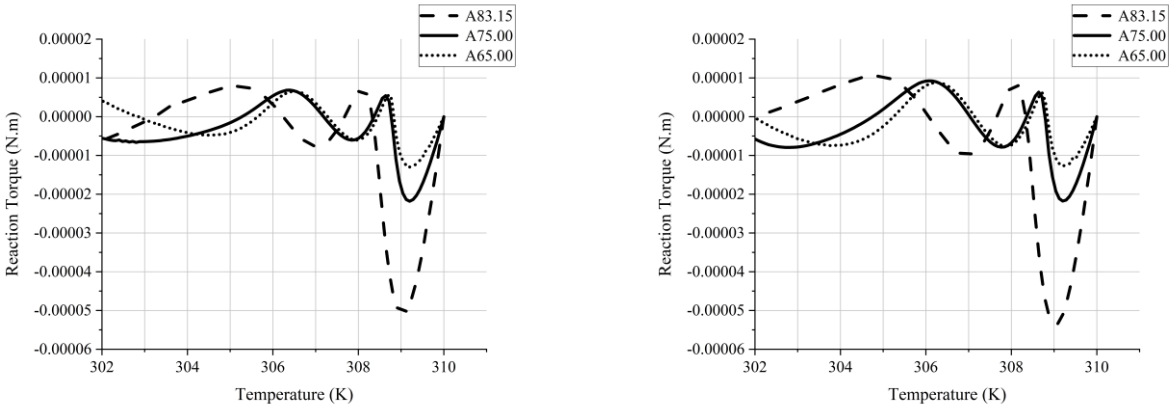

(a) (b)

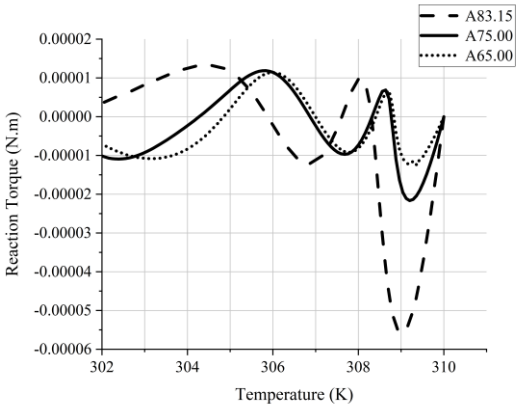

(c)

Figure 12. Reaction torque of an actuator with *NxH1.50Azz.zzVP50.00* and with two constrained ends for (a) *N3*, (b) *N4*, and (c) *N5*

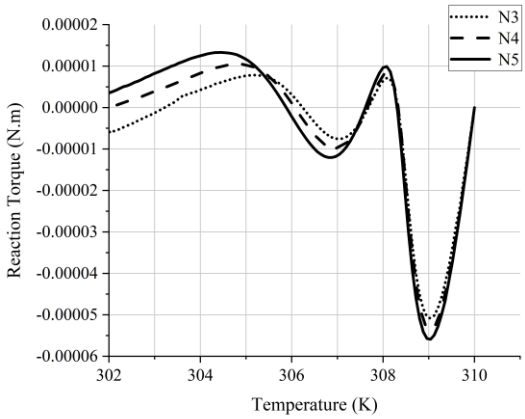

Figure 13. Reaction torque of the actuator with *N3H1.50A83.15VP50.00* for (a) *N3*, (b) *N4*, and (c) *N5*

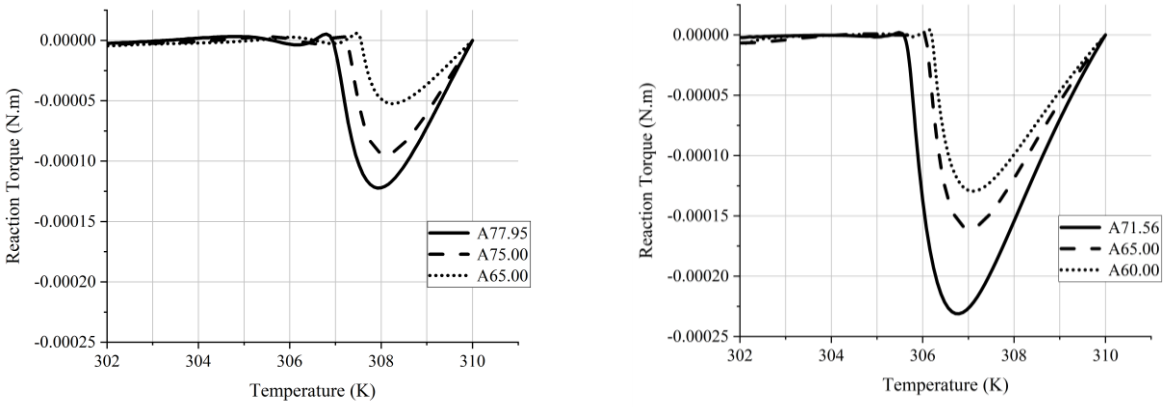

1(a) (b)

Figure 14. Effect of angle α on the reaction torque of the twisting actuator with *N3Hy.yyAzz.zzVP50.00* for dimensions of (a) *H2.00*, and (b) *H2.50*

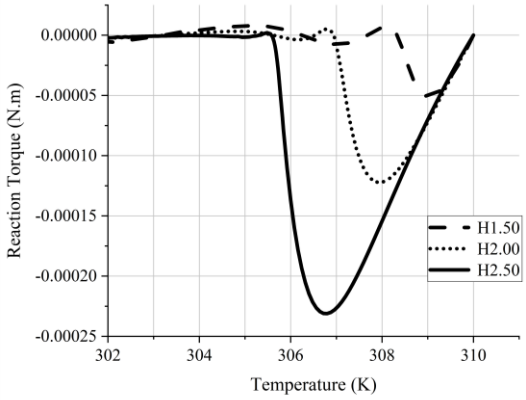

Figure 15. Reaction torque of the actuator with *N3Hy.yyAzz.zzVP50.00* for different sizes of the actuator. The interface line passes through corners of the actuator.

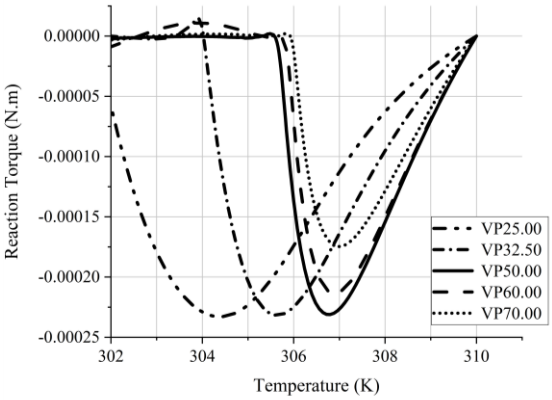

Figure 16. Reaction torque of the actuator with *N3H2.50A71.56VPww.ww* for different volumetric percentages of hydrogel.

Amir Ghasemkhani was born in 1993 in Hamedan, Iran. He obtained his BS and MS degree from the Department of Mechanical Engineering at Bu-Ali Sina University, Iran, Hamedan, in 2020. His research interests include Computational Mechanics, Soft Materials, Constitutive Modelling and Fluid Solid-interaction Analysis of Hydrogels. He analytically and numerically investigated on various hydrogel-based sensors/actuators with different sensitivities to environmental conditions such as temperature, pH, and light. Moreover, participating in a project for deriving constitutive equations for photo-thermal sensitive hydrogel was another great experience in his career.

Hashem Mazaheri received his BS, MS and PhD degrees in Mechanical Engineering from the Department of Mechanical Engineering at Sharif University of Technology, Tehran, Iran, in 2007, 2010 and 2015, respectively. He is now an Associate Professor in the Department of Mechanical Engineering at Bu-Ali Sina University, Iran, Hamedan. His research interests include Computational Mechanics, Nonlinear Finite Element Method, Smart Hydrogels Constitutive Modelling, and Numerical-experimental Analysis of Composite Structures.

Pouya Beigzadeh Arough is an engineer deeply passionate about sustainable energy solutions. Graduating from Bu-Ali Sina University in 2019, he worked on his bachelor's thesis under the supervision of his professor, Dr. Hashem Mazaheri, focusing on smart materials like hydrogels. Since then, his field of work has evolved, and he is currently pursuing a master's in energy engineering at the University of Genoa (since 2021), where his focus has shifted towards energy systems and optimization. His research interests extend to energy systems, green hydrogen, fuel cells, and optimization techniques, showcasing his commitment to advancing clean energy technologies.